Extreme Loading® for Structures

Version 3.1

Corrosion Effects Option

April 2010

1. Introduction

Corrosion of gusset plates was identified as one of the main causes for failure in the catastrophic collapse of the Minnesota I-35 Bridge. This tragedy triggered a national awareness of the inspection of existing bridges for corrosion and other deterioration factors to ensure that the bridges can carry their design loads. With tens of thousands of bridges to be inspected, a versatile tool that can take into account the effects of corrosion is very important so that engineers can decide the bridge's new capacity and whether it needs rehabilitation or not. Click the link below to view Applied Science International's (ASI) analysis of the Minnesota I-35 Bridge:
http://www.appliedscienceint.com/upload/ShowCases/PDF/Forensic-Analysis-of-the-Minnesota-I-35-Bridge-Failure.pdf

In the new release of Extreme Loading® for Structures Software (ELS), Version 3.1, ASI, has added new and powerful feature that allows engineers to consider the effects of corrosion while analyzing structures.

With the added corrosion effects feature, the ELS user will be able to:

1- Determine the new capacity of the corroded structure.

2- Determine the corrosion ratio at which a bridge may fail

3- For corroded bridges, determine the new capacity after strengthening the bridge with FRP or other strengthening factors.

The area reduction due to the effects of corrosion can be applied to pre-stressing tendons, steel or composite sections. With automatic considerations of cracking, plastic hinges and failure mechanism, ELS is the only commercially available tool that makes it easy for bridge engineers to do such analysis of the bridge's current status to decide whether it needs rehabilitation or not and study the effectiveness of a strengthening strategy. This document illustrates these powerful features through two case studies, for RC and steel bridges subjected to the effects of corrosion.

2. Examples

In this document, we will validate the rust option where the behavior of a rusted reinforced concrete pre-stressed girder and a rusted Steel box section where the effect of the rust on the load carrying capacity of the members are going to be discussed.

2.1. Reinforced Concrete Example

Fig. 1 shows a simply supported pre-stressed beam subjected to a 3 point loading [Ref. 1]. Dimensions and loading setup are shown in Fig. 1. Fig. 2 shows the ELS model for the girder where half the girder is hidden to show the reinforcement and pre-stressed tendon inside the model. A pre-stressing Force of 40.5 kips (180 KN) was applied to the tendons.

The compressive strength of the concrete is 6.26 ksi(0.0431 kN/mm^2), while the yielding stress of the steel reinforcement is 64.97 ksi(0.45 kN/mm^2). The yielding stress of the tendons is 196 ksi (1.35 kN/mm^2).

To show the ELS capabilities; first a verification of the model will be done by analyzing the beam under the applied load and compare it with the experimental results. Then rusting will be applied on the whole length of the pre-stressed tendon by 50%. Finally, an analysis of the same girder will be preformed by applying the same rust then warp the section with FRP plates.

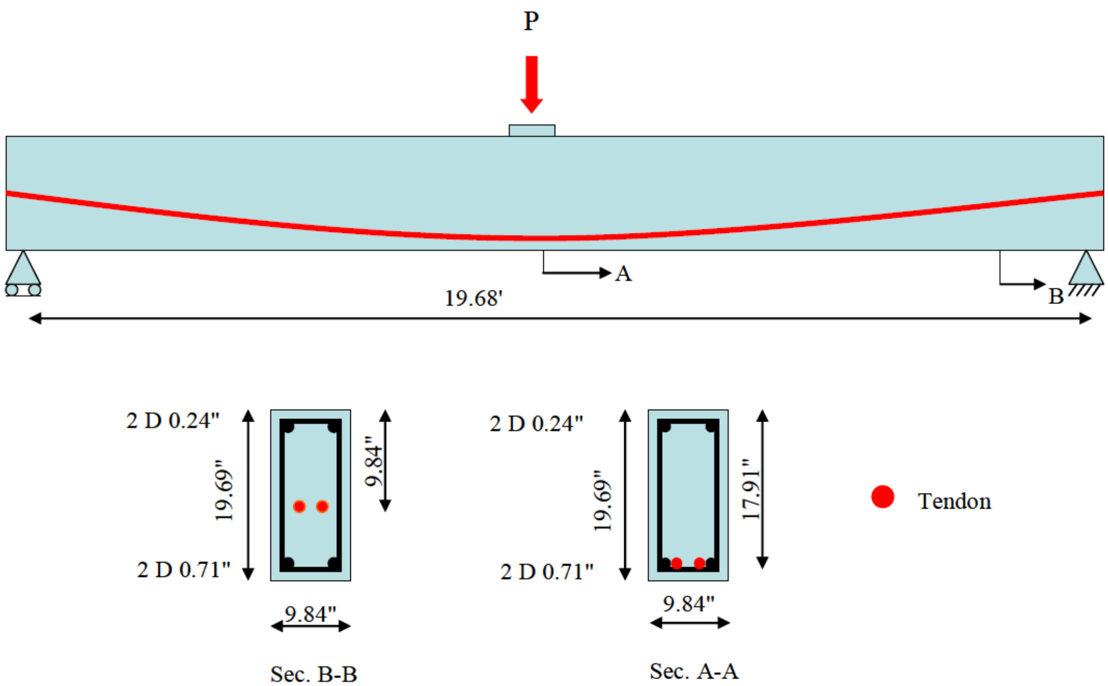

Fig. 1 Pre-Stressed Reinforced Concrete Girder

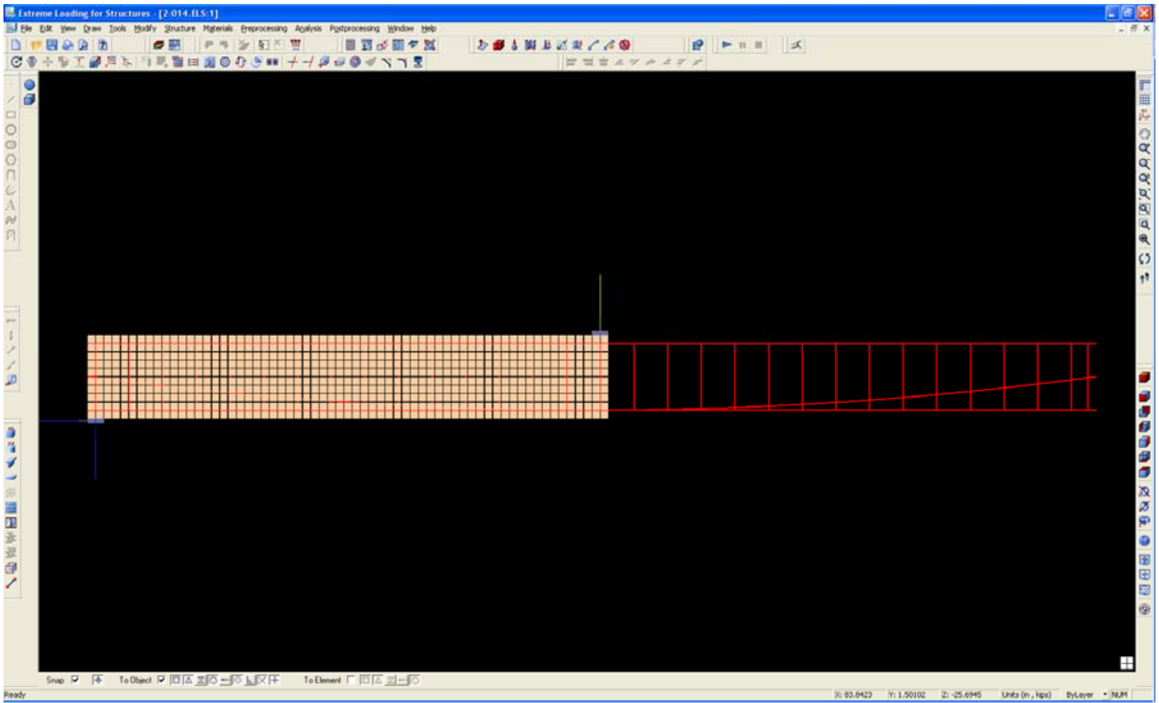

Fig. 2 ELS Model

2.1.1. Behavior before applying the rust effects

The analysis is performed using two loading staged. In the first stage, the own weight and pre-stressing forces are applied in 10 increments to follow possible cracking and nonlinear behavior in this stage. Then in stage II, the concentrated load is applied as incremental displacement load at the center of the girder as shown in Fig. 2. Fig. 3 illustrates the Moment-Deflection analytical results compared to the experimental ones. As can be seen, the results are close to the experiments. Fig. 4 shows the load deflection curve where it can be seen that the failure load recorded was 61 Kips. Referring to Fig. 4, the girder first deflected upward due to the pre-stressing forces then it started deflecting downward when the concentrated load was applied. The behavior is well predicted in the elastic stage and in the post cracking stage. Fig. 5 shows the calculated principal strain contours. The principal strains represent a good, obvious representation of crack localizations. Fig. 6 shows the observed experimental cracking pattern of the beam. The experimental cracks are generally in a good agreement with the ELS results. It should be noted that the cause of failure is a compression failure happened near the loading point as shown in Fig. 7

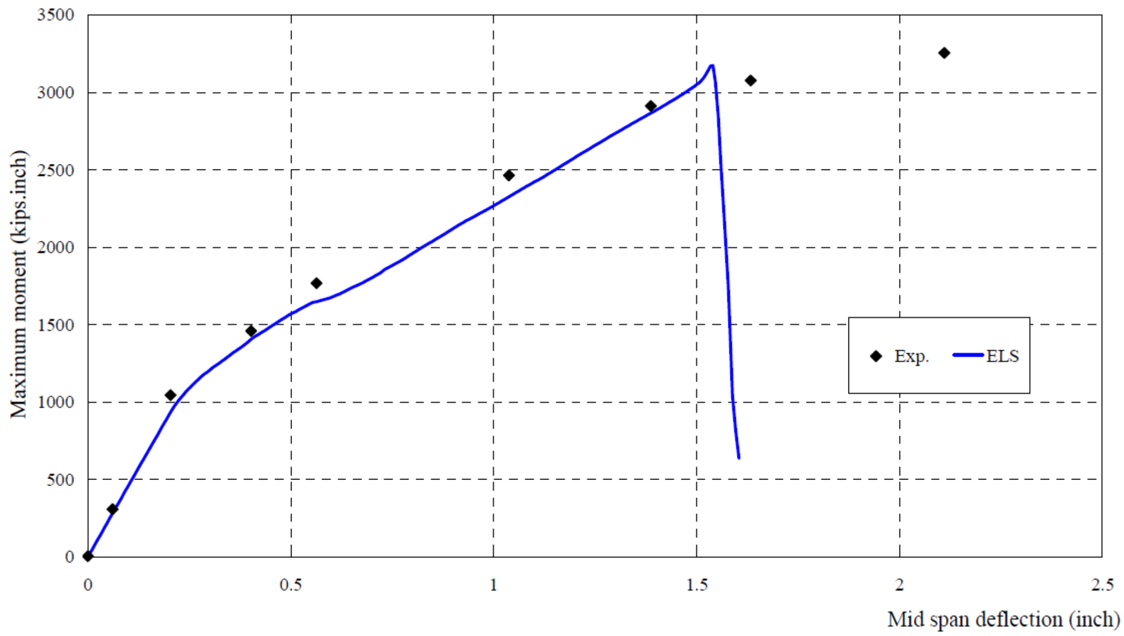

Fig. 3 Moment Deflection Predicted by ELS in a Comparison to Experimental Results

Fig. 4 Load Deflection Predicted by ELS

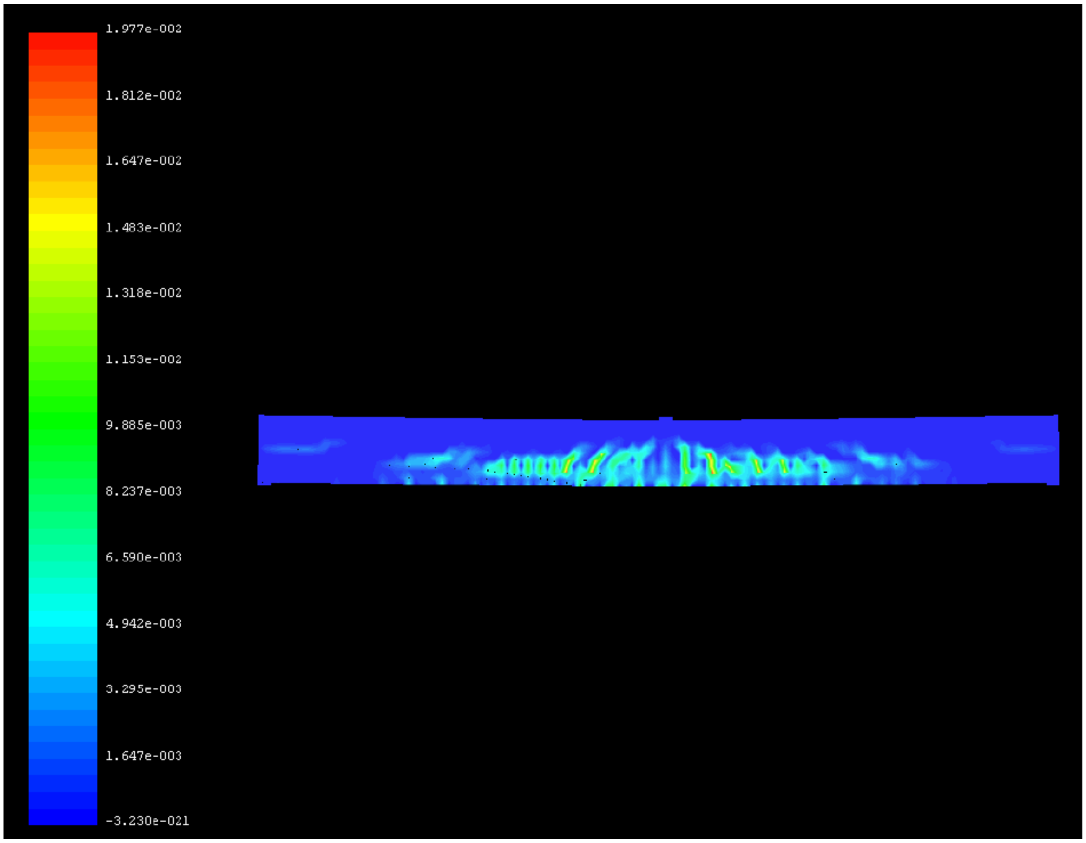

Fig. 5 Principal strain contours predicted by ELS

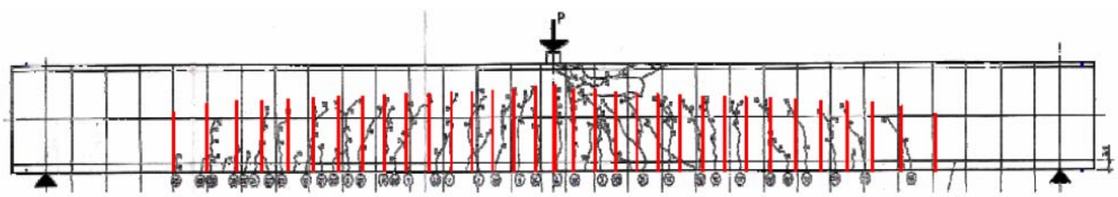

Fig. 6 Observed experimental cracking pattern

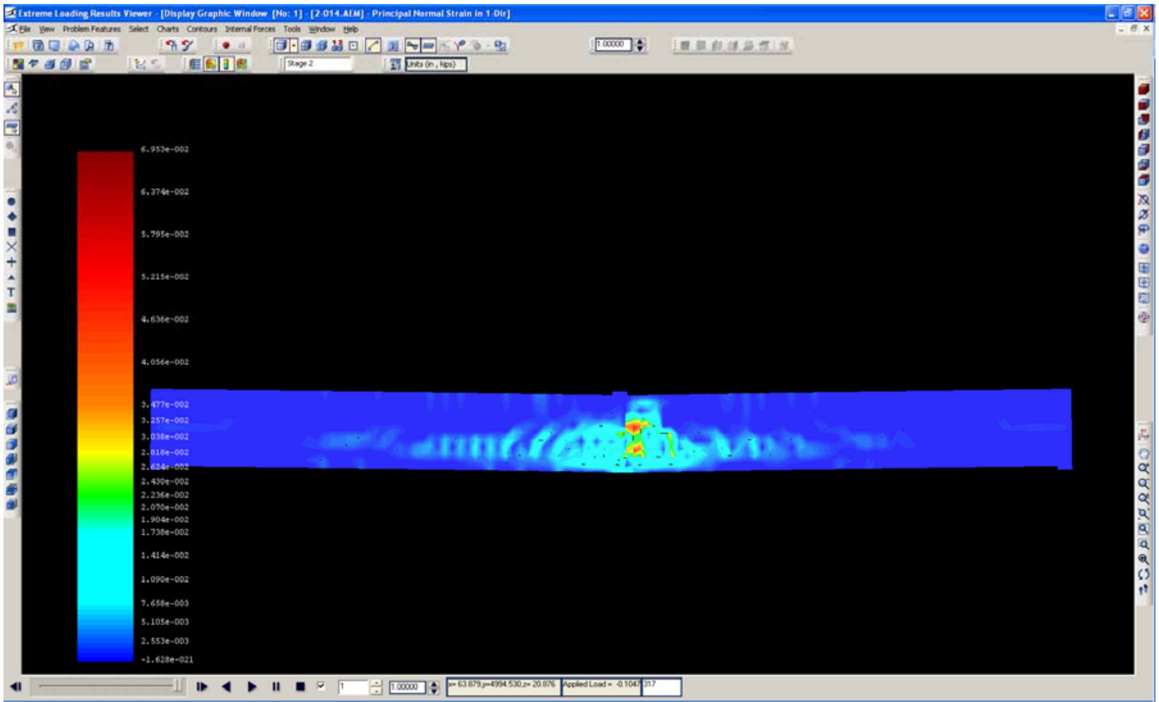

Fig. 7 Compression failure in the girder

2.1.2. Behavior after applying the rust

Fig. 8 shows the load deflection curve for the girder after applying rust on the pre-stressed tendon by 25% which means that the area of the tendon was reduced by 25%. This load deflection curve passed through different stages. From point (1) to point (2) the own weight and the pre-stressing force were applied. At point (2) the loading begin to increase incrementally until it reaches point (3) where the rust begins to appear. The rust (area reduction) was applied from point (3) up to (4) by gradually reducing the rebar area in 90 steps. Then the loading was increased incrementally until the girder reaches its ultimate capacity and failed at load 51Kips. A compression failure also occurred in this case as shown in Fig. 9. Fig. 10 shows a comparison between the load deflection before and after applying rust. It is clear that the rust caused decrease in the load carrying capacity of the section which leads to early failure.

It should be emphasized that in nonlinear analysis, applying the rust changes from the beginning of the analysis may lead to inaccurate results since the sequence of loading is a critical factor using nonlinear analysis while it is not a factor using linear analysis.

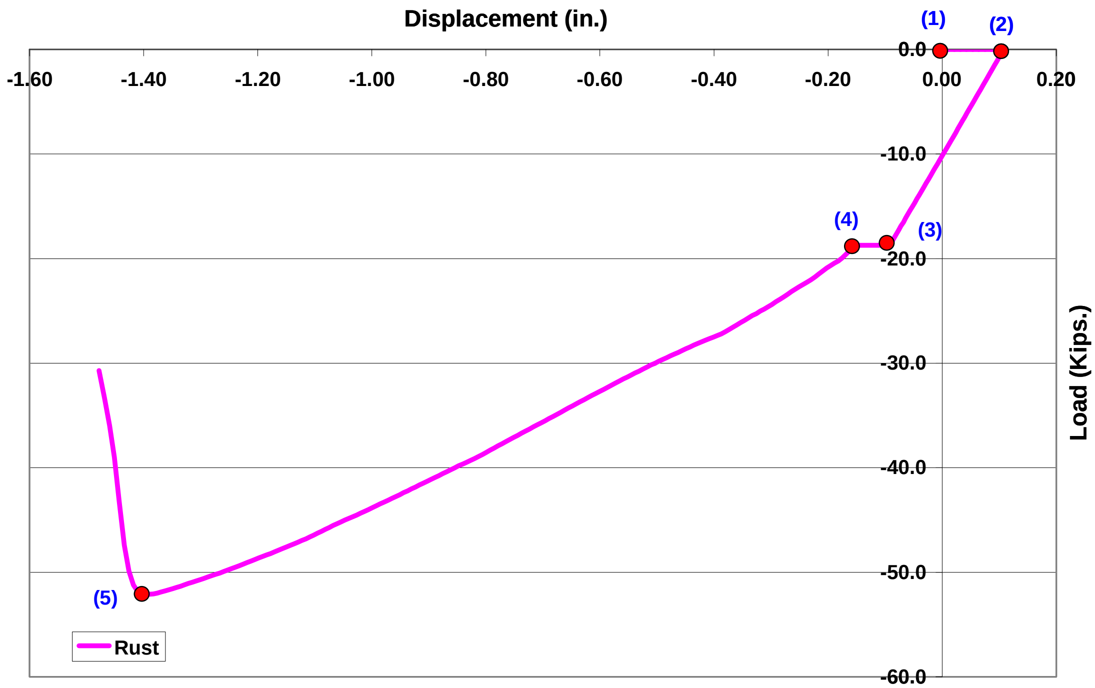

Fig. 8 Load Deflection Predicted by ELS

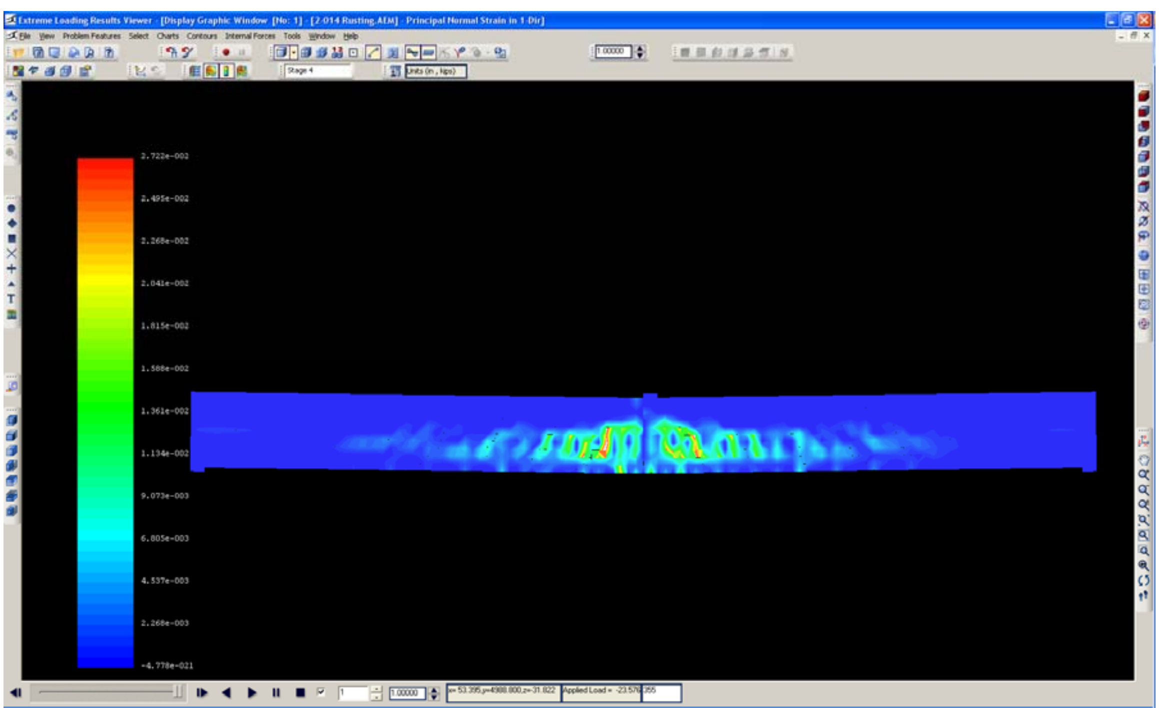

Fig. 9 Compression failure near loading point

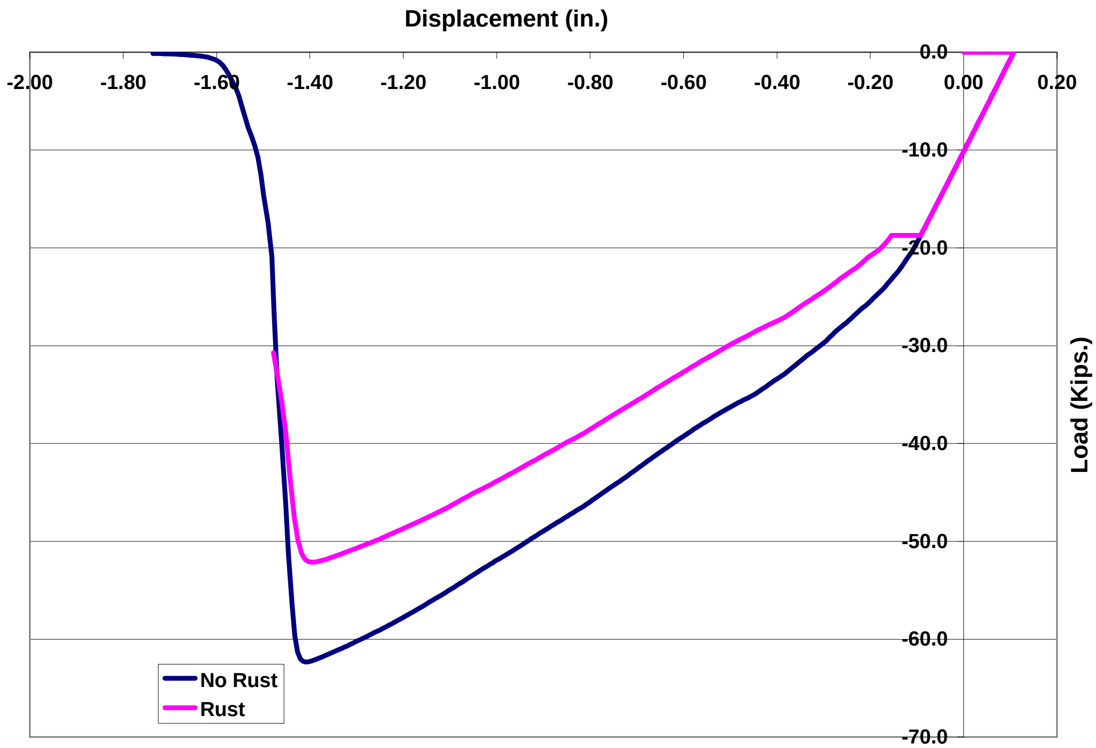

Fig. 10 Load Deflection Predicted by ELS

2.1.3. Behavior after apply the rust then strengthening by FRP plates

To show the capabilities of ELS, the analysis will be applied in the following staged loadings:

1- Apply own weight and pre-stressing loads (Segment 1-2 at Fig. 12 below)

2- Then loads will be applied to the girder (Segment 2-3)

3- Then the load will be kept constant and the rusting will be applied to the rebar (Segment 3-4). The girder deflection increases due to rust while the rust is applied.

4- Then the load is applied again to the rusted girder (Segment 4-5)

5- Before reaching the failure load, the girder will be retrofitted with FRP plates having a thickness of 0.5mm on both sides of the girder as shown in Fig. 11.

6- The load is applied again until it reaches the ultimate capacity of the section at about 80Kips (Point 6).

Fig. 13 shows the failure of the retrofitted girder. Fig. 14 shows a comparison between different rusting cases.

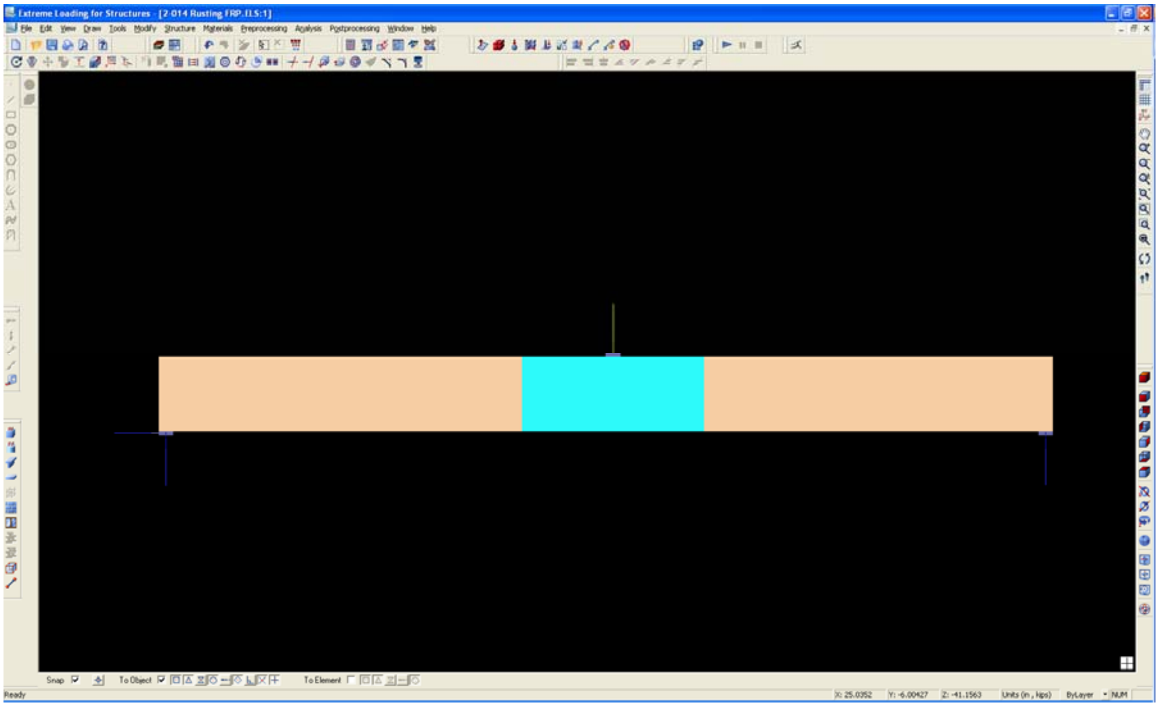

Fig. 11 Girder Retrofitted by FRP Plates

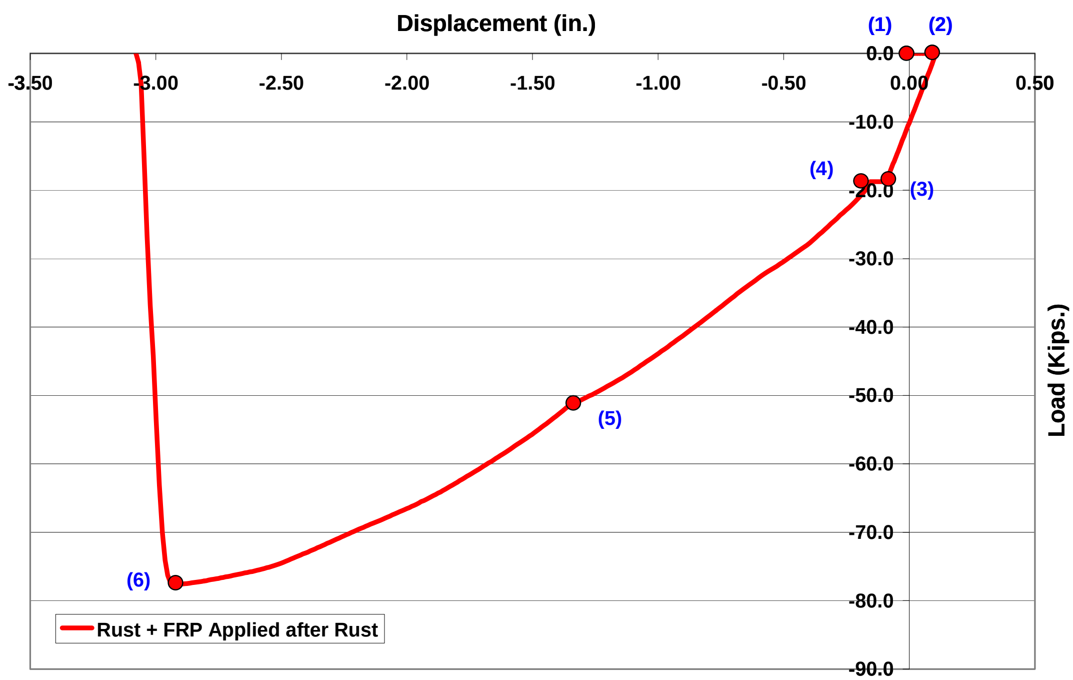

Fig. 12 Load deflection curve for Girder Retrofitted by FRP Plates

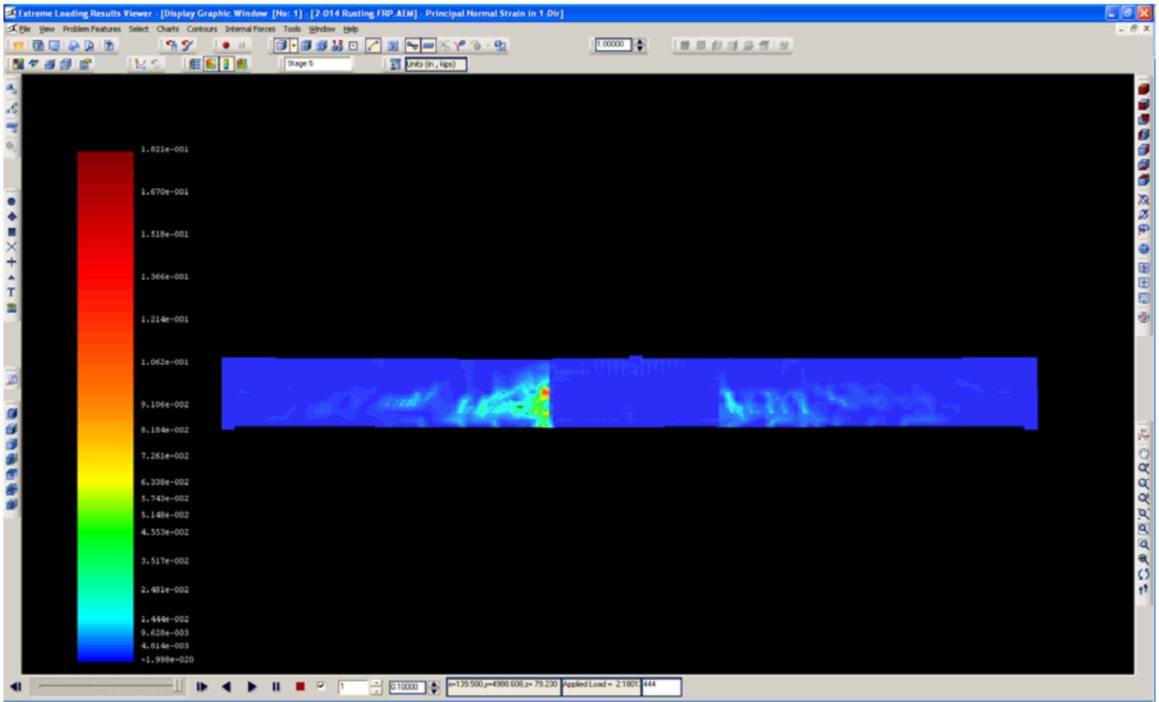

Fig. 13 Compression failure near the end of the FRP plates

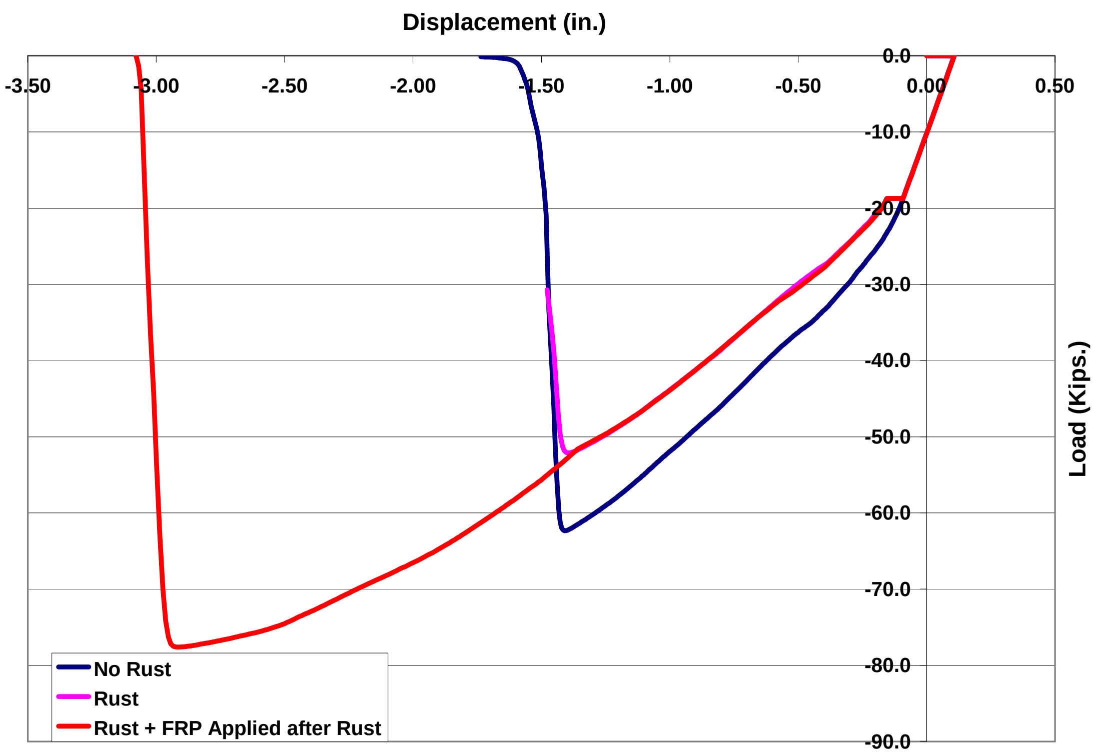

Fig. 14 Comparison between different rusting cases

In this example, the ELS power can be summarized in the following key points:

1- Multi staged loading
2- Multi staged construction (Adding FRP plates in the middle of the analysis then continue loading)
3- Applying pre-stressing loads
4- Applying rust effects even to the pre-stressing tendons or any other steel bars or sections.
5- Calculating crack initiation, propagation till reaching the failure loads.
6- Finally, this case was built, analyzed by an engineer not a scientist.

2.2. Steel Example

Fig. 15 shows a steel frame that is subjected to in-plane lateral loading at one of its corners (upper-left corner) [Ref. 2]. The geometry, the dimensions, the element sections and the loading pattern are shown in Fig. 15. Fig. 16 shows the ELS model. The steel yield stress is 34 ksi (0.24 kN/mm^2) and the young's modulus is 28777 ksi (196.2 kN/mm^2).

To demonstrate the capabilities of ELS, this example will be solved twice; the first time lateral loads are going to be applied on the original frame. The second time rusting will be applied need the columns end near the bottom beam connection.

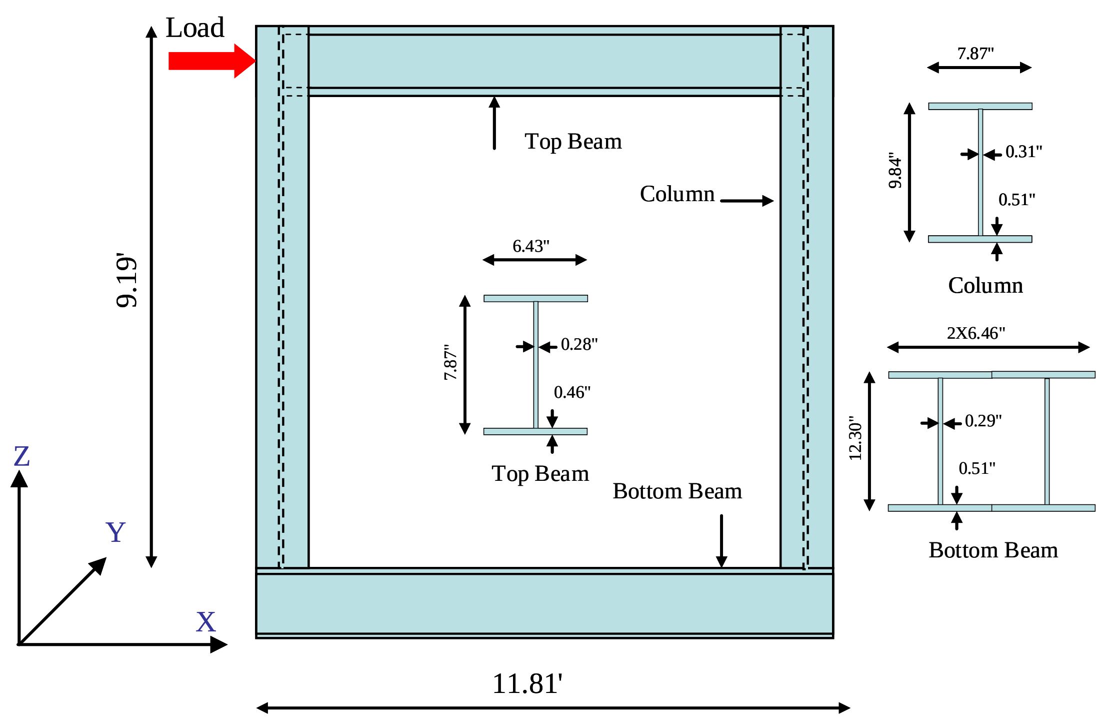

Fig. 15 Steel frame subjected to lateral loads

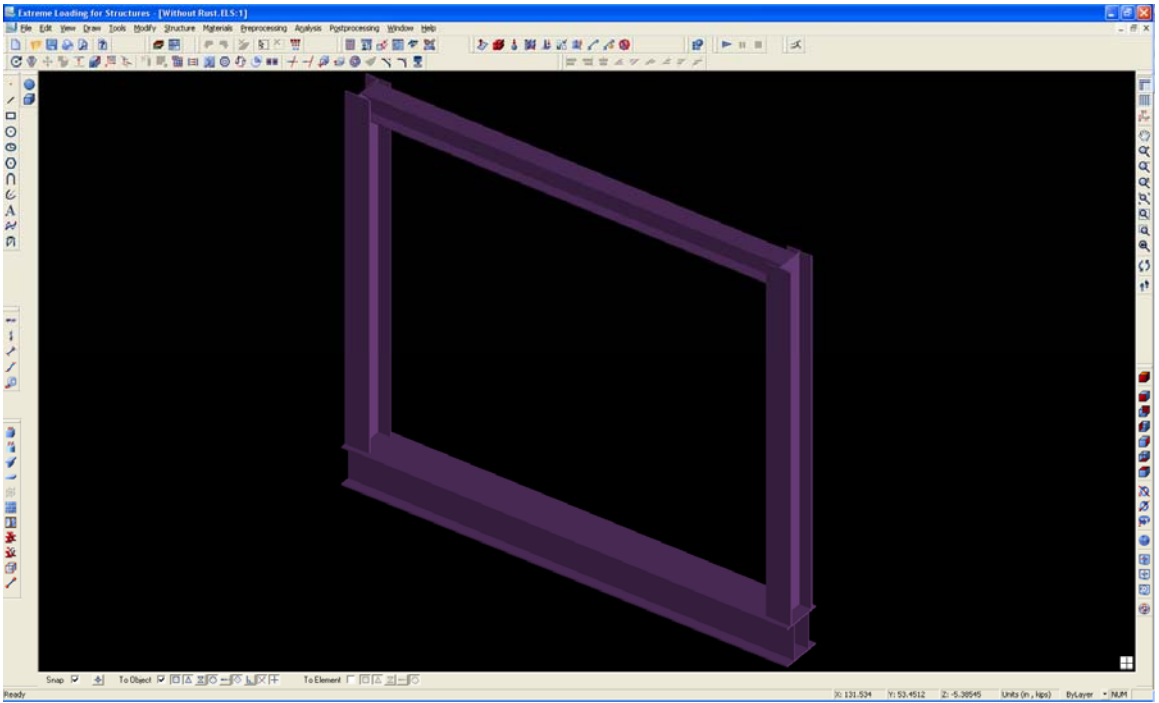

Fig. 16 ELS model

2.2.1. ***Behavior before applying the rust***

Fig. 17 shows the deformed shape for the frame as well as the B.M.D. Fig. 18 shows the load deflection curve predicted by ELS.

The load is applied in two stages; the own weight stage followed by the application of the lateral loads.

Referring to Fig. 18; the steel reaches its yield strength then continue deformation after formation of the plastic hinges at all connections. It should be emphasized that using ELS, the formation of plastic hinges is automated without any user intervention or definition of when or where the hinges will be in effect.

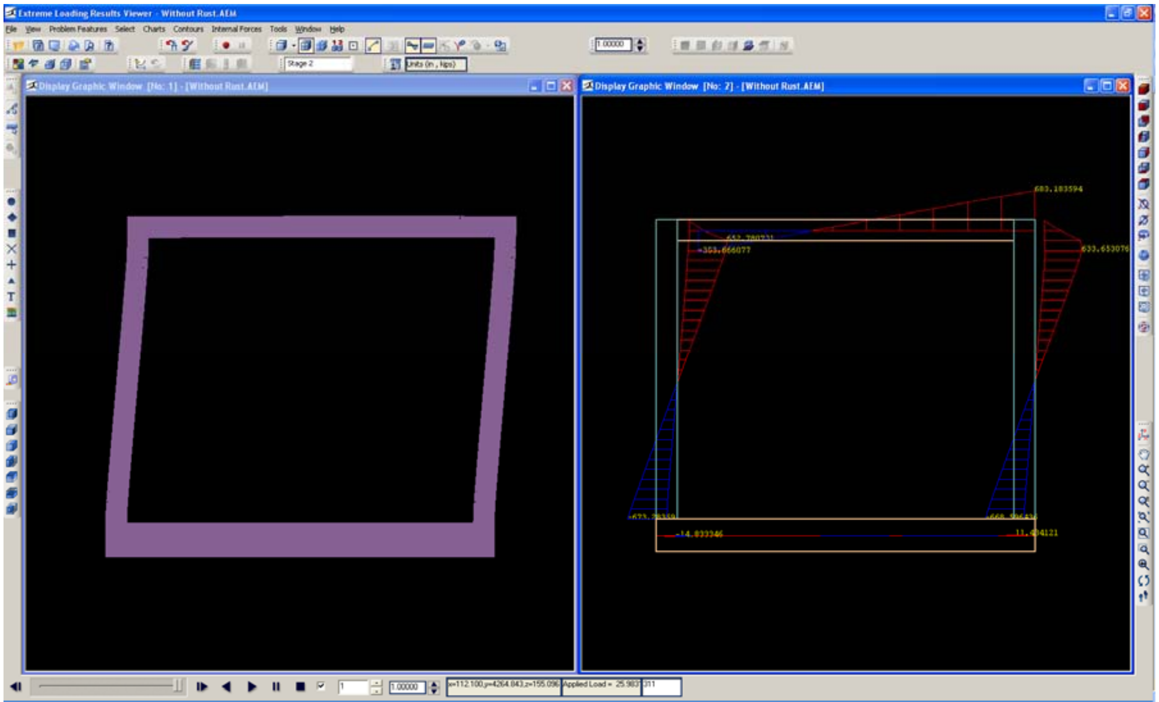

Fig. 17 Deformed shape and B.M.D for the frame

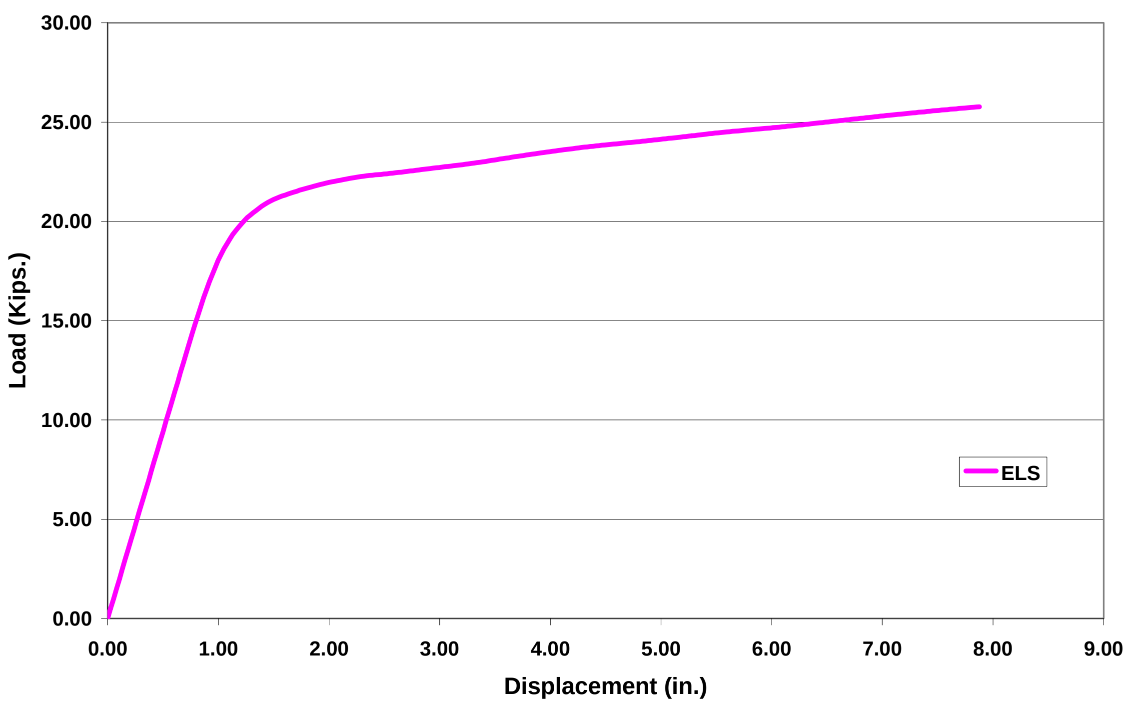

Fig. 18 Load Deflection curves comparison between ELS and experimental data

2.2.2. Behavior after applying the rust

Fig. 19 shows the ELS model for the frame with the rust applied near the bottom beam. The percent of rust is 50%. Fig. 20 shows the load deflection curve predicted by ELS. The load deflection curve passes through deferent stages as follows:

1- In stage 1, the own weight is applied followed by lateral displacement loading (Segment 1-2). The frame deflection is linear.

2- When the deflection reaches to point (2) the rusting begins to take effect and the load was kept constant.

3- From point (2) to point (3) the deflection increases due to rust until it reaches to point (3). It is obvious from the load deflection curves was linear before reaching point (2) and it becomes nonlinear at point 3. This is due to the reduction of the cross sectional area of the rusted region.

4- At point (3), the load begins to increase incrementally until the analysis stops at point (4). Fig. 21 shows the B.M.D in the columns at point (2) while Fig. 22 shows the B.M.D in the columns at point (3). Fig. 23 shows the B.M.D at point (4). Note that the bending moment values decreased due to rust from point (2) to Point (3) then it increased again until point (4).

Fig. 24 shows the moment deflection curve at the rusted connection predicted by ELS. It is clear that the bending moment reduced from point (2) to point (3) where the rust effects ends while the displacement kept increasing. Referring to Fig. 21 and Fig. 22, the bending moment at the lower rusted connection is reduced due to rust effects while the bending moment at the top un-rusted connection increased since the lower connection becomes weaker. Fig. 25 shows a compression between the load deflection curves ELS results without rust and ELS results with rust.

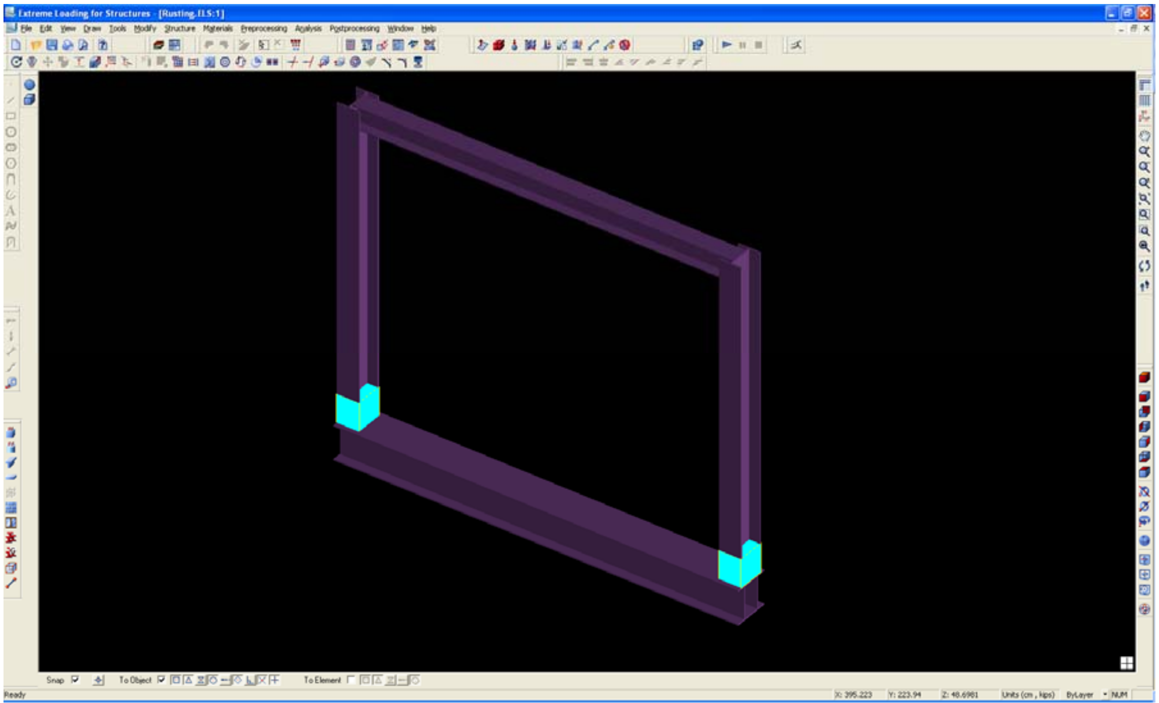

Fig. 19 ELS Model for steel frame with rust

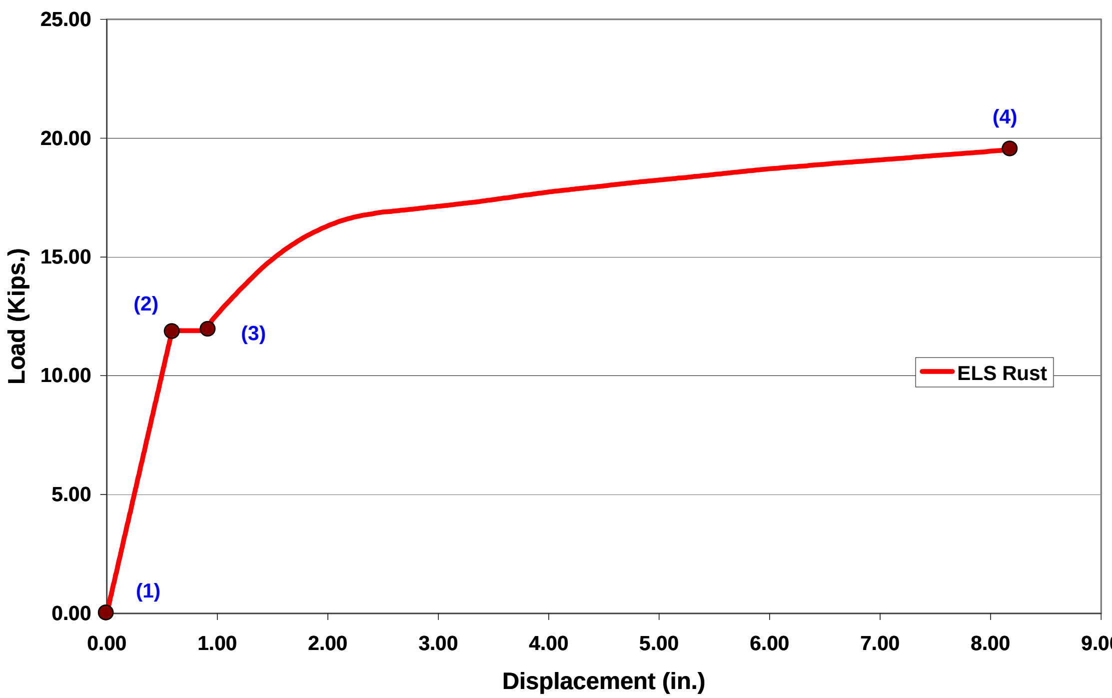

Fig. 20 Load Deflection curve predicted by ELS for rusted frame

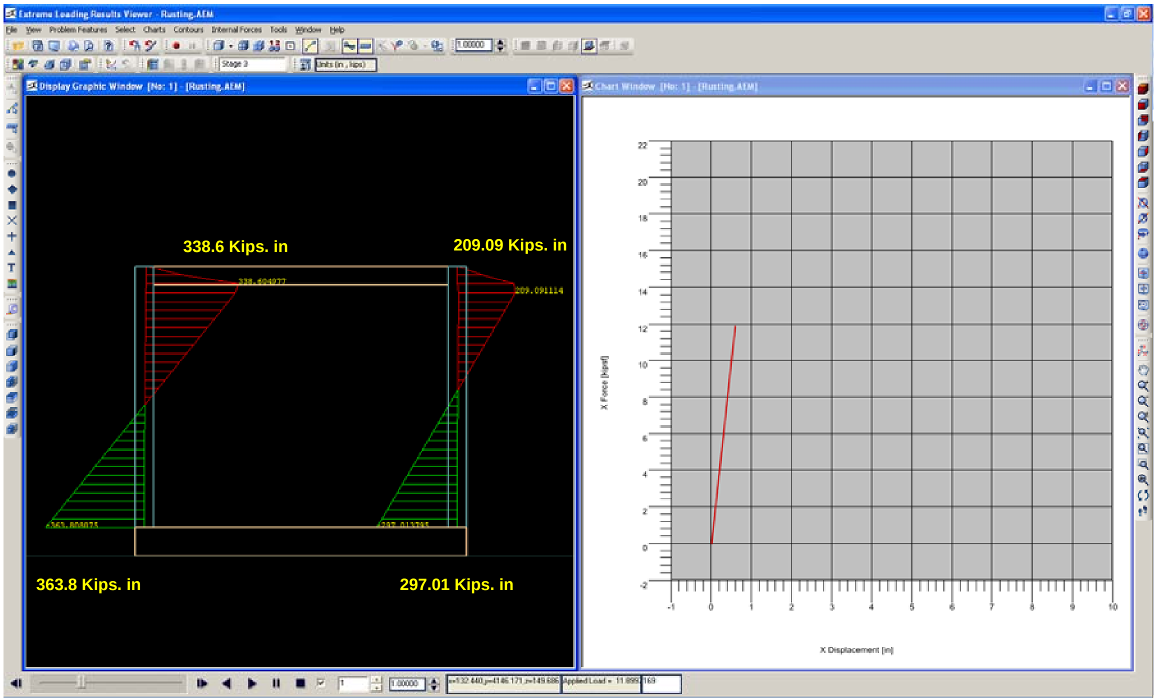

Fig. 21 B.M.D at point (2)

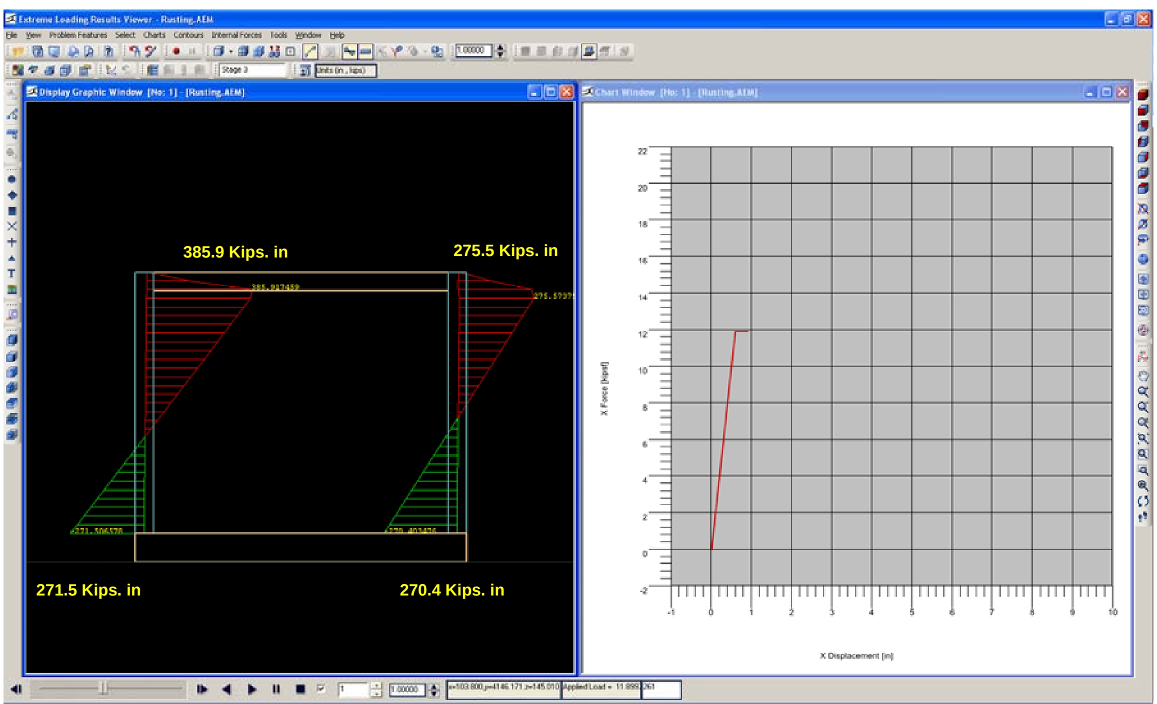

Fig. 22 B.M.D at point (3)

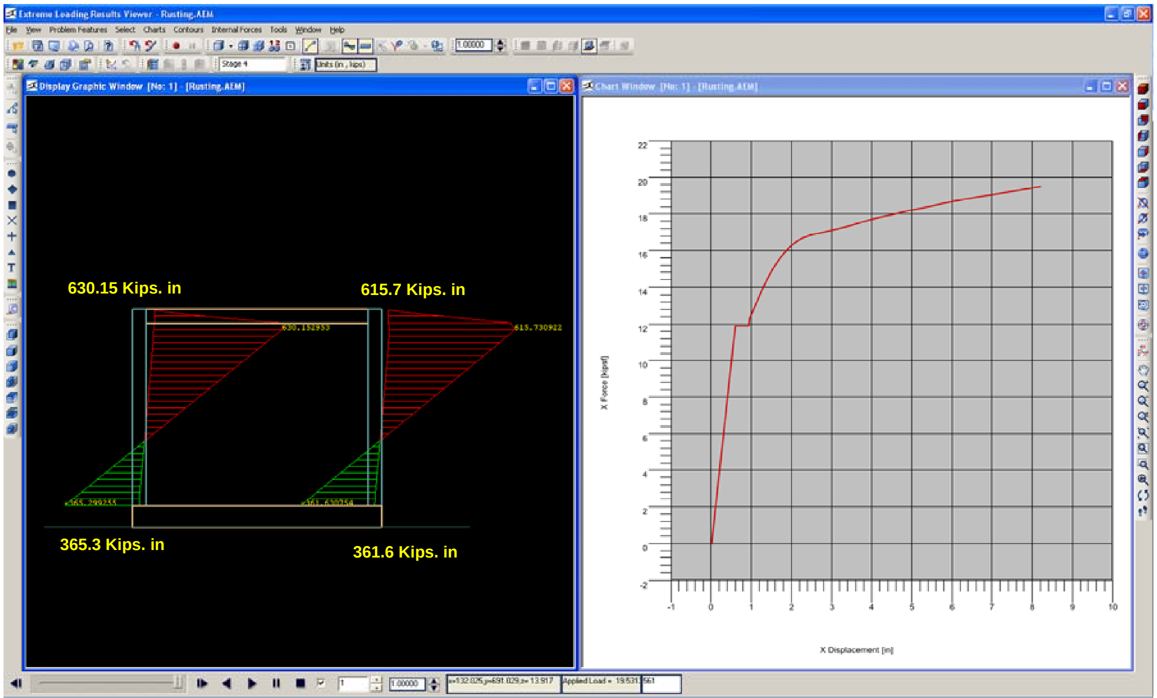

Fig. 23 B.M.D at point (4)

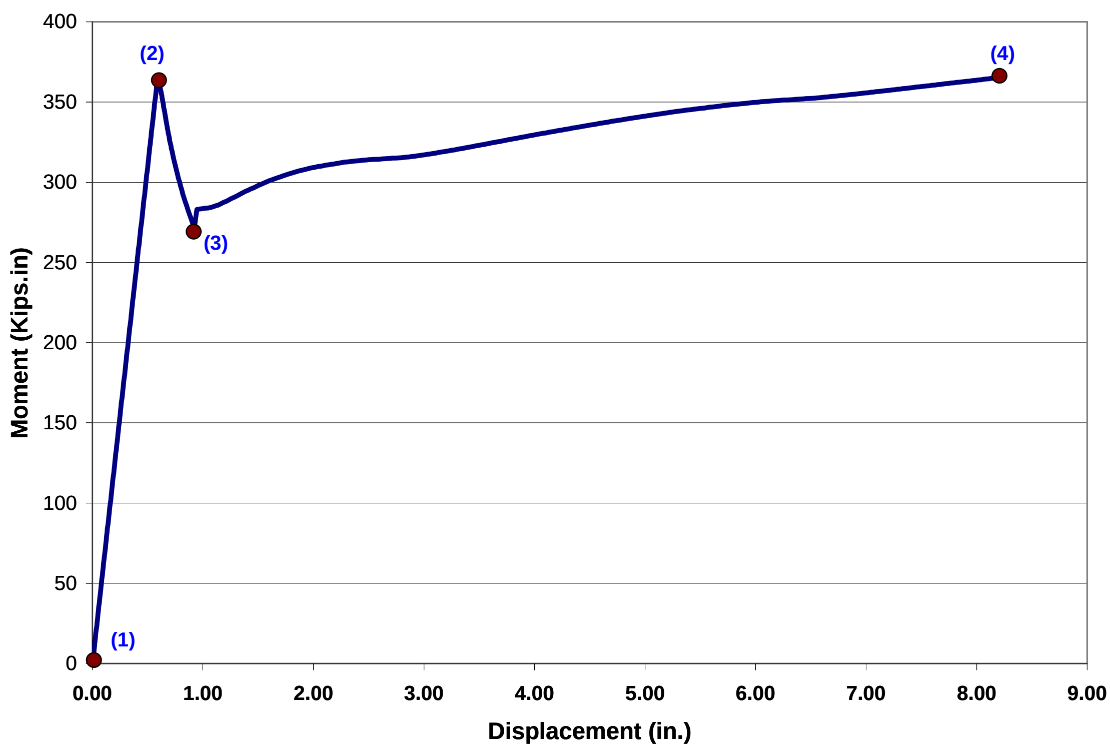

Fig. 24 Moment Deflection curve predicted by ELS

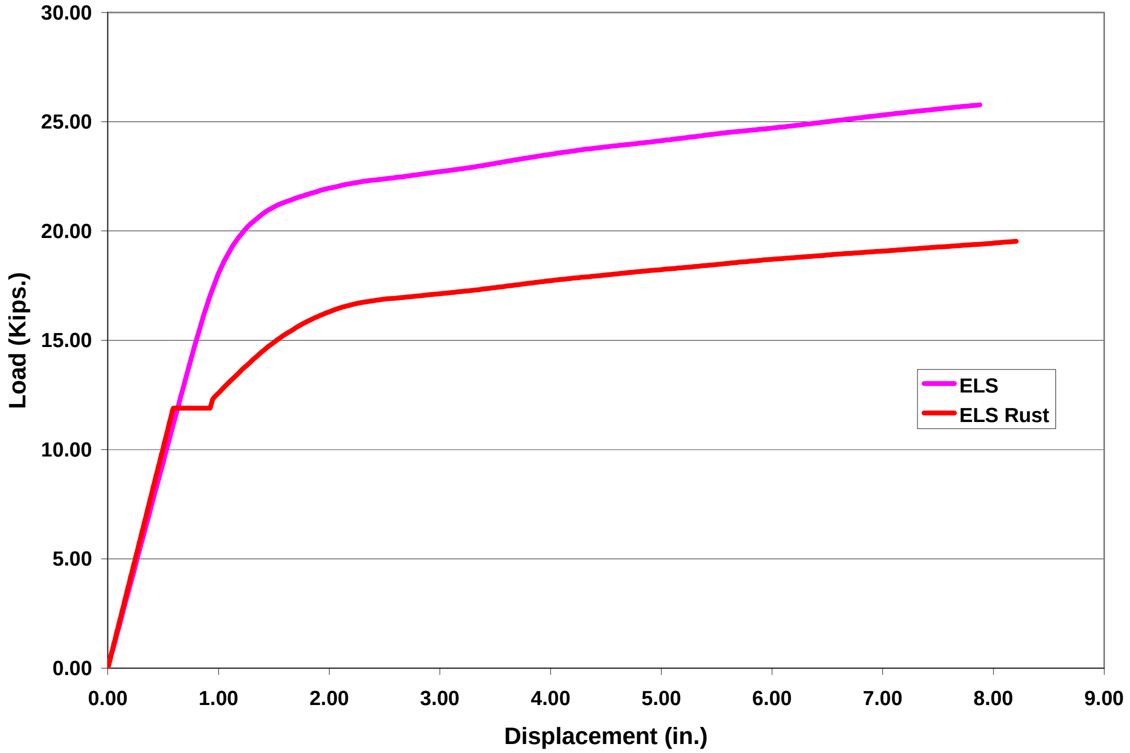

Fig. 25 Moment Deflection curve predicted by ELS

3. References

1. Mark Rebentrost, “Deformation Capacity and Moment Redistribution of Partially Pre-stressed beams”, Department of Civil and Environmental, Adelaide University, Australia.

2. Richardson, J. (1986), "The behavior of masonry in filled steel frames', M.Sc. Thesis, University of New Brunswick, Fredericton, N.B., Canada.

3. Technical Manual of Extreme Loading for Structures.